Ruthenium dithiophosphates: synthesis, X-ray crystal structure, spectroscopic and electrochemical properties

Prateek U. Jain [a], Pradip Munshi [a], Mrinalini G. Walawalkar [a], Sankar Prasad Rath [b], Kajal Krishna Rajak [b], Goutam Kumar Lahiri [a,*]

[a] *Department of Chemistry, Indian Institute of Technology, Bombay, Powai, Mumbai 400076, India*
[b] *Department of Inorganic Chemistry, Indian Association for the Cultivation of Science, Jadavpur, Calcutta 700032, India*

Abstract

The reactions of ammonium salts of dialkyldithiophosphate ligands, $(RO)_2PS_2^-NH_4^+$ (R = Me/Et), with $Ru^{III}Cl_3 \cdot 3H_2O$ in methanol solvent and under N_2 atmosphere result in one-electron paramagnetic tris complexes $\{(RO)_2PS_2\}_3Ru^{III}$ (**1**) in the solid state. The molecular structures of both complexes were determined by single-crystal X-ray diffraction. This shows the expected pseudo-octahedral geometry with reasonable strain due to the presence of a four-membered chelate ring. The reflectance spectra of the solid complexes display two bands in the range 596–476 nm and in the solid state the complexes exhibit one isotropic EPR signal at 77 K. Although the complexes **1** are stable in the solid state, in solution the complexes are transformed selectively into the diamagnetic and electrically non-conducting sulfur-bridged dimetallic species $[\{(RO)_2PS_2\}_2Ru^{IV}(\mu\text{-}S)_2Ru^{IV}\{S_2P(OR)_2\}_2]$. The formation of dimeric species in the solution state is authenticated by the electrospray mass spectrum of one representative complex where R = Et (**1b**). In dichloromethane solution the complexes show two moderately strong sulfur to ruthenium charge-transfer transitions in the range 514–419 nm, and two strong ligand based transitions in the UV region. The complexes exhibit two successive reversible reductions in the ranges $1.01 \rightarrow 0.91$ V and $-0.44 \rightarrow -0.49$ V versus SCE corresponding to Ru^{IV}–Ru^{IV}/Ru^{III}–Ru^{III} and Ru^{III}–Ru^{III}/Ru^{II}–Ru^{II} couples respectively. Electrochemically or chemically generated first step reduced complexes $[\{(RO)_2PS_2\}_2Ru^{III}(\mu\text{-}S)_2Ru^{III}\{S_2P(OR)_2\}_2]^{2-}$ display two ligand to metal charge-transfer transitions in the visible region and in the complexes the two one-electron paramagnetic metal centers (low-spin Ru^{III}, t_{2g}^5, $S = 1/2$) are antiferromagnetically coupled. The second step reduced species $[\{(RO)_2PS_2\}_2Ru^{II}(\mu\text{-}S)_2Ru^{II}\{S_2P(OR)_2\}_2]^{4-}$ are observed to be very unstable.

Keywords: Ruthenium; Phosphates; X-ray crystal structures

1. Introduction

Although the ruthenium chemistry of dithioacid based ligands such as dithiocarbamate and dithiocarbonate has been the subject of continuous study [1–24], the corresponding ruthenium dithiophosphate chemistry has not been developed much [25–29]. The versatile bonding, structural features as well as fascinating chemical and electrochemical reactivities of ruthenium dithiocarbamate and dithiocarbonate complexes have prompted us to make a systematic study of ruthenium dialkyldithiophosphate complexes. The present study indicates that the reactions of ammonium salts of dialkyldithiophosphates, $(RO)_2P(S)S^-NH_4^+$, with $RuCl_3 \cdot 3H_2O$ result in tris complexes $\{(RO)_2PS_2\}_3Ru^{III}$ (**1**) in the solid state, whereas in solution the complexes **1** exist predominantly in the dimeric form of type $[\{(RO)_2PS_2\}_2Ru^{IV}(\mu\text{-}S)_2\text{-}Ru^{IV}\{S_2P(OR)_2\}_2]$. Herein we report the solid state characterization of the tris complexes **1**, including the single-crystal X-ray structure and the solution spectroscopic and electron-transfer properties of the complexes.

2. Experimental

2.1. Materials

Commercial ruthenium trichloride (S.D. Fine Chemicals, Bombay, India) was converted into $RuCl_3 \cdot 3H_2O$ by repeated evaporation to dryness with concentrated hydrochloric acid. The ligands NH_4L^{1-2} were synthesized according to the reported method [30]. Other chemicals and solvents were

reagent grade and were used as received. Silica gel (60–120 mesh) used for chromatography was of BDH quality. For spectroscopic and electrochemical studies, HPLC grade solvents were used. Commercial tetraethyl ammonium bromide was converted into pure tetraethyl ammonium perchlorate by following an available procedure [31].

2.2. Physical measurements

UV–Vis spectra were recorded using a Shimadzu-160 spectrophotometer. FT-IR spectra were taken on a Nicolet spectrophotometer with samples prepared as KBr pellets. Solution electrical conductivity was checked using a Systronic 305 conductivity bridge. Magnetic susceptibility was checked with a PAR vibrating sample magnetometer. NMR spectra were obtained with a 300 MHz Varian Fourier transform spectrometer. Cyclic voltammetric, differential pulse voltammetric and coulometric measurements were carried out using a PAR model 273A electrochemistry system. Platinum wire working and auxiliary electrodes and an aqueous saturated calomel reference electrode (SCE) were used in a three-electrode configuration. The supporting electrolyte was $[NEt_4]ClO_4$ and the solute concentration was 10^{-3} M. The half-wave potential E^0_{298} was set equal to $0.5(E_{pa}+E_{pc})$, where E_{pa} and E_{pc} are the anodic and cathodic cyclic voltammetric peak potentials respectively. A platinum wire-gauze working electrode was used in coulometric experiments. All experiments were carried out under a dinitrogen atmosphere and were uncorrected for junction potentials. The electrospray mass spectra were recorded on a Micromass Quattro II triple quadrupole mass spectrometer. The elemental analyses were carried out with a Carlo Erba (Italy) elemental analyzer. The EPR measurements were made with a Varian model 109C E-line X-band spectrometer fitted with a quartz Dewar for measurements at 77 K (liquid nitrogen). The spectra were calibrated using tetracyanoethylene (tcne) ($g=2.0023$).

2.3. Preparation of complexes

The complexes (**1a** and **1b**) were synthesized by following a general procedure. Details are given for the complex **1a**. Yields vary in the range 70–75%.

2.3.1. Tris(dimethyldithiophosphate)ruthenium(III) (*1a*)

$RuCl_3\cdot 3H_2O$ (100 mg, 0.38 mmol) was dissolved in 15 ml of methanol solvent and a stream of nitrogen gas was flushed through the solution for a period of 15 min. The ligand NH_4L^1, 266 mg (1.52 mmol), was added and the reaction mixture was stirred magnetically under nitrogen atmosphere for 12 h. The solvent was removed under reduced pressure and the solid product thus obtained was purified using a silica gel column. On elution with benzene one pink colored band was separated out, leaving behind a dark mass at the top of the column which did not move even on using methanol. On removal of benzene under reduced pressure, dark crystalline solid complex **1a** was obtained in the pure state. Yield 190 mg (72%).

2.4. X-ray structure determination

Single crystals of complexes **1a** and **1b** were grown by slow diffusion of dichloromethane solution of the complexes into hexane followed by slow evaporation.

Cell parameters were determined by least-squares fit of 25 ($2\theta=10$–$17°$) and 30 ($2\theta=15$–$30°$) machine centered reflections for **1a** and **1b** respectively. Data were collected by the ω-scan technique in the ranges $4\le 2\theta\le 50°$ and $3\le 2\theta\le 48°$ on a Nonius MACH 3 and Siemens R3m/V four-circle diffractometer for **1a** and **1b** respectively with graphite-monochromated Mo Kα radiation ($\lambda=0.71073$ Å) at 293 K. Significant crystal data and data collection parameters are listed in Table 1. The check reflections were measured after every 100 reflections during data collection to monitor crystal stability. No significant intensity reduction was observed during exposure to X-ray radiation. Absorption correction was done by performing psi-scan measurements for **1a** and for **1b** all data were corrected for Lorentz polarization effects and empirical absorption corrections were done on the basis of azimuthal scans of six reflections [32]. For **1a**, data reduction was done using MAXUS and structure solution and refinement were done using the programs SHELXS-97 and SHELXL-97 respectively [33,34]. For **1b**, all calculations for data reduction, structure solution and refinement were done using the program SHELXTL Version 5.03 [33,34]. The metal atom was located from the Patterson map and the other non-hydrogen atoms emerged from successive Fourier synthesis and the structure was refined by full-matrix least-squares on F^2. All non-hydrogen atoms were refined anisotropically. Hydrogen atoms were included in calculated positions. The numbers of variable parameters were 198 and

Table 1
Crystallographic data for complexes **1a** and **1b**

	1a	**1b**
Formula	$C_6H_{18}O_6P_3S_6Ru$	$C_{12}H_{30}O_6P_3S_6Ru$
FW	572.54	656.70
Crystal symmetry	monoclinic	monoclinic
Space group	*Cc*	*C*2/*c*
a (Å)	14.121(6)	14.267(6)
b (Å)	11.191(10)	13.569(3)
c (Å)	12.978(7)	14.316(6)
β (°)	97.11(10)	90.33(3)
U (Å^3)	2035.4(2)	2771(2)
Z	4	4
D_c (Mg m^{-3})	1.868	1.574
μ(Mo Mα) (mm^{-1})	1.638	1.214
R_1 [a]	0.0221	0.0378
wR_2 [b]	0.0565	0.0985

[a] $R_1=\sum||F_o|-|F_c||/\sum|F_o|$.
[b] $wR_2=[\sum\{w(F_o^2-F_c^2)^2\}/\sum\{w(F_o^2)^2\}]^{1/2}$; $w^{-1}=\sigma^2(F_o^2)+(ap)^2+bp$, where $p=(F_o^2+2F_c^2)/3$ and *a* and *b* are respectively 0.0389, 0.0551 and 1.6585, 5.2552 for **1a** and **1b**, constant adjusted by the program.

128, affording data-to-parameter ratios of 9.47:1 and 17.05:1 for **1a** and **1b** respectively. The refinement converged to $R_1 = 0.0221$, $wR_2 = 0.0565$ and $R_1 = 0.0378$, $wR_2 = 0.0985$ and goodness of fit 1.070 and 1.064 with the largest difference peak of 0.399 and 0.559 e $Å^{-3}$ near the metal atom for **1a** and **1b** respectively.

3. Results and discussion

3.1. Synthesis

Two dialkyldithiophosphate ligands were used for the present study and are abbreviated as NH_4L^1 and NH_4L^2.

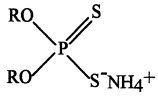

R= Me, NH_4L^1
R= Et, NH_4L^2

The reaction of NH_4L with $RuCl_3 \cdot 3H_2O$ in methanol solvent under N_2 atmosphere at room temperature for 12 h results in a dark solution. Chromatographic purification of the dark solution on silica gel column, using benzene as eluant, yields pure tris complexes, $Ru^{III}\{S_2P(OR)_2\}_3$ (**1**) (R = Me **1a**, R = Et **1b**) in the solid state, Eq. (1).

$$Ru^{III}Cl_3 \cdot 3H_2O + (RO)_2PS_2NH_4 \rightarrow Ru^{III}\{S_2P(OR)_2\}_3 + NH_4Cl + H_2O \quad (1)$$

3.2. Solid state characterization

The complexes **1a** and **1b** are stable in the solid state. Microanalytical data of the complexes are in good agreement with the calculated values (Table 2). The complexes are one-electron paramagnets (Table 2), as expected for low-spin Ru^{III} complexes (low spin d^5, $S = 1/2$) [35].

The molecular structures of both the complexes were determined by single-crystal X-ray diffraction. The crystal structures are shown in Figs. 1 and 2. Selected bond lengths and angles are listed in Table 3. The complexes are monomeric and the lattice consists of one type of molecule where the

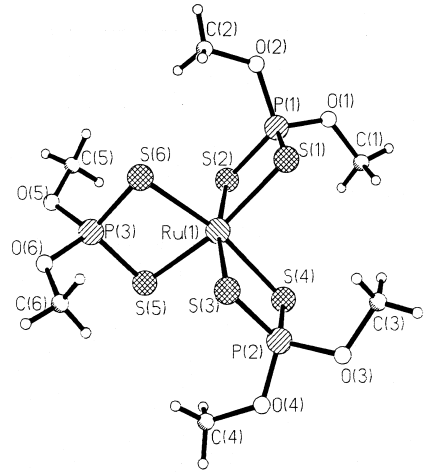

Fig. 1. An ORTEP plot for complex **1a**.

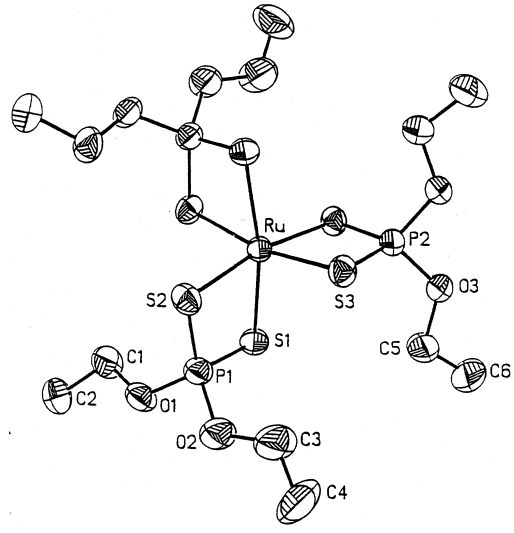

Fig. 2. An ORTEP plot for complex **1b**.

dialkyldithiophosphate ligands are in bidentate *S,S* mode. For **1b**, Ru and P_2 atoms are in special positions and a mirror plane passes through them (Fig. 2). The RuS_6 coordination sphere is distorted octahedral as can be seen from the angles subtended at the metal (Table 3). The observed distortion from the perfect octahedral symmetry originates from the constraints due to the four-membered chelate rings in which the average S–Ru–S bite angles are 81.54(8)° and 81.84(6)° for **1a** and **1b** respectively (Table 3). A similar effect of ring

Table 2
Microanalytical [a], reflectance [b], magnetic moment [c] and EPR data [d] for complexes **1**

Compound	Elemental analysis (%)		Reflectance λ (nm)	Magnetic moment μ_M (BM)	EPR (g)
	C	H			
1a	12.49 (12.59)	3.19 (3.15)	580, 476	2.059	2.030
1b	22.14 (21.95)	4.53 (4.57)	596, 476	1.916	1.865

[a] Calculated values are in parentheses.
[b] In the solid state.
[c] In the solid state at 298 K.
[d] In the solid state at 77 K.

Table 3
Selected bond distances (Å) and angles (°) and their estimated standard deviations for **1a** and **1b**

	1a	**1b**	
Ru–S(1)	2.433(3)	2.407(2)	
Ru–S(2)	2.402(3)	2.4249(14)	
Ru–S(3)	2.419(3)	2.4011(13)	
Ru–S(4)	2.452(3)		
Ru–S(5)	2.395(3)		
Ru–S(6)	2.408(3)		
S(1)–P(1)	1.994(5)	1.996(2)	
S(2)–P(1)	2.011(4)	1.997(2)	
S(3)–P(2)	1.987(4)	2.000(2)	
P(1)–O(1)	1.525(9)	1.564(3)	
P(1)–O(2)	1.618(8)	1.569(4)	
P(2)–O(3)	1.624(8)	1.571(3)	
S(1)–Ru–S(2)	81.62(10)	S(1)–Ru–S(2)	81.63(5)
S(3)–Ru–S(4)	81.17(10)	S(3)#1–Ru–S(3)	82.06(7)
S(5)–Ru–S(6)	81.83(4)	S(1)#1–Ru–S(2)	91.01(5)
S(5)–Ru–S(2)	90.74(11)	S(2)–Ru–S(2)#1	95.84(7)
S(2)–Ru–S(6)	98.67(13)	S(3)–Ru–S(1)	98.32(5)
S(5)–Ru–S(3)	96.65(12)	S(1)–Ru–S(1)#1	169.04(7)
S(2)–Ru–S(3)	169.32(4)	S(3)#1–Ru–S(2)#1	91.73(5)
S(6)–Ru–S(3)	90.03(11)	S(3)#1–Ru–S(2)	168.76(5)
S(5)–Ru–S(1)	168.98(12)	S(3)–Ru–S(1)#1	89.97(5)
S(6)–Ru–S(1)	91.43(12)	P(1)–S(2)–Ru	86.62(6)
S(3)–Ru–S(1)	92.04(11)	P(1)–S(1)–Ru	87.13(6)
S(5)–Ru–S(4)	91.20(11)	P(2)–S(3)–Ru	86.97(7)
S(6)–Ru–S(4)	168.10(12)	S(1)–P(1)–S(2)	104.53(8)
S(1)–Ru–S(4)	96.84(4)	S(3)–P(2)–S(3)#1	104.00(10)
S(2)–Ru–S(4)	91.01(11)	O(1)–P(1)–O(2)	94.9(2)
		O(3#1)–P(2)–O(3)	96.2(3)

constraints on the molecular geometry has been also observed earlier [36–39].

The Ru–S distances are unequal, the longer and shorter distances are respectively 2.452(3) and 2.395(3) Å for **1a** and 2.425(14) and 2.401(13) Å for **1b**. The Ru^{III}–S distances in the present complexes are reasonably longer than the corresponding Ru^{III}–S distances, 2.376(4) and 2.383(6) Å (mean Ru^{III}–S distances) in the tris-ruthenium dithiocarbamate complexes $Ru^{III}(S_2CNEt_2)_3$ and $Ru^{III}\{S_2C(CN)(CH_2)_4O\}_3$ respectively [40,41] (the only two other structurally characterized tris-ruthenium(III) dithioacid complexes).

The distances within the dithiophosphate ligands agree well with those found in structurally characterized dithiophosphate complexes of other metal ions [42–44].

It may be noted that the present work demonstrates the first crystal structure of a ruthenium complex incorporating the dithiophosphate ligand.

The reflectance spectra of the solid complexes **1** exhibit two broad bands in the visible region (Fig. 3, Table 2). The band profiles look similar for both complexes, but the lowest energy band maxima are observed to be sensitive to the nature of the R groups.

Consistent with the low-spin configuration, the complexes $[Ru^{III}L_3]$ (low-spin d^5 Ru^{III}, $S=1/2$) display one isotropic

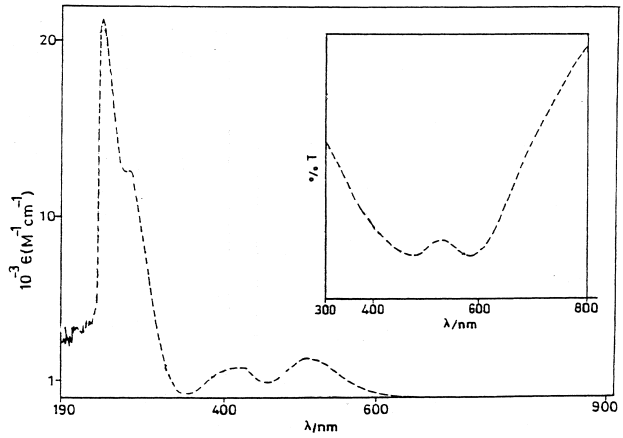

Fig. 3. Electronic spectrum of **1a** in dichloromethane. The inset shows the reflectance spectrum of **1a**.

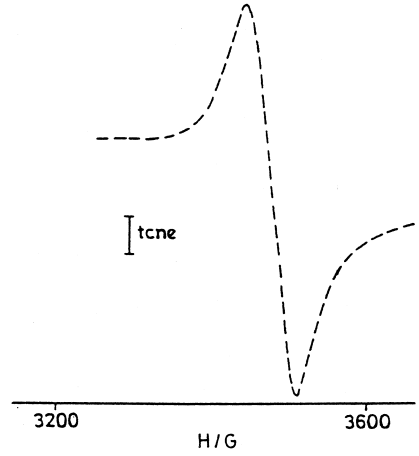

Fig. 4. X-band EPR spectrum of **1b** in the solid state at 77 K.

broad EPR signal (Table 2, Fig. 4) [45,46]. No anisotropic pattern has been observed even at liquid N_2 temperature (77 K).

3.3. Solution properties of the complexes

The solid complexes **1** are fairly soluble in non-polar solvents such as dichloromethane, chloroform and benzene, but are sparingly soluble in polar solvents such as acetonitrile, *N,N*-dimethylformamide and dimethylsulfoxide. In dichloromethane and acetonitrile the complexes **1** are non-conducting, diamagnetic and consequently EPR silent even at chloroform–toluene glass temperature (77 K, liquid N_2). The change in magnetic behavior of the complexes while moving from the solid to solution state implies that the one-electron paramagnetic solid complexes **1** undergo molecular reorganization in the solution state which eventually leads to the formation of diamagnetic complexes.

The electrospray mass spectrum of a representative complex (**1b**) was recorded in dichloromethane solvent. The maximum molecular peak is observed at *m/z* 1006 (Fig. 5) which corresponds to the molecular ion $[\{(EtO)_2PS_2)\}_2Ru^{IV}(\mu\text{-}S)_2Ru^{IV}\{S_2P(OEt)_2\}_2]$ (calculated molecular

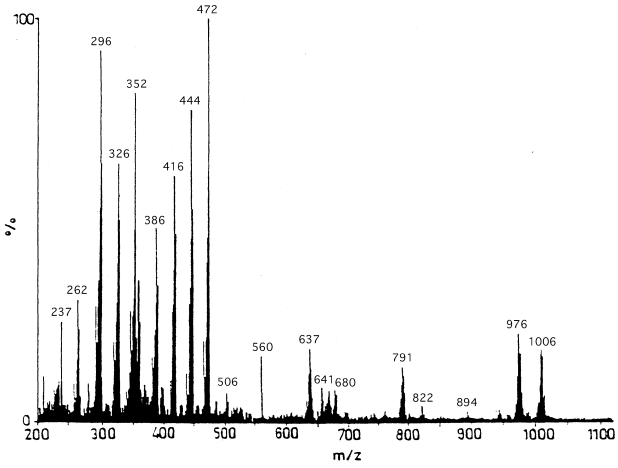

Fig. 5. Electrospray mass spectrum of $[\{(EtO)_2PS_2\}_2Ru^{IV}(\mu\text{-}S)_2\text{-}Ru^{IV}\{S_2P(OEt)_2\}_2]$ (**1b**) in dichloromethane.

weight 1006.2). Thus the tris complexes **1** in the solid state have been transformed into the sulfur bridged dinuclear species as shown in Scheme 1. The conversion of solid tris complexes **1** to the dimeric complexes in the solution state can account for the change in magnetic behavior (one-electron paramagnetic in the solid state and diamagnetic in the solution state) and overall electron balancing.

It may be noted that the tris dithiophosphate cobalt complex $Co^{III}(L)_3$ is also known to liberate one L^- from the tris core in the solution state and the liberated L^- subsequently dimerizes to the disulfide species [47].

^{1}H NMR spectra of the ligands NH_4L^{1-2} and the complexes were recorded in D_2O and $CDCl_3$ respectively. The representative spectra are shown in Fig. 6. The ^{1}H NMR spectrum of NH_4L^1 exhibits two singlets at 3.663 and 3.615 ppm due to two inequivalent $-OCH_3$ groups and similarly NH_4L^2 exhibits two quartets (3.93 and 3.76 ppm) and two triplets (1.17 and 1.12 ppm) due to two inequivalent $-OC_2H_5$ groups. The ^{1}H NMR spectrum of the $R = CH_3$ complex exhibits one

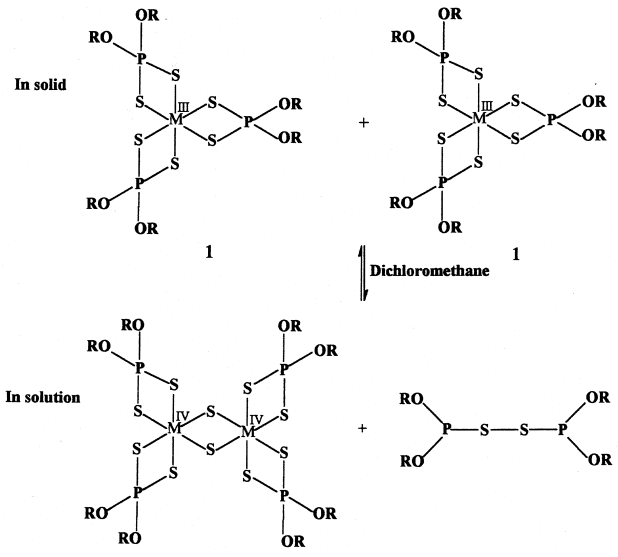

Scheme 1.

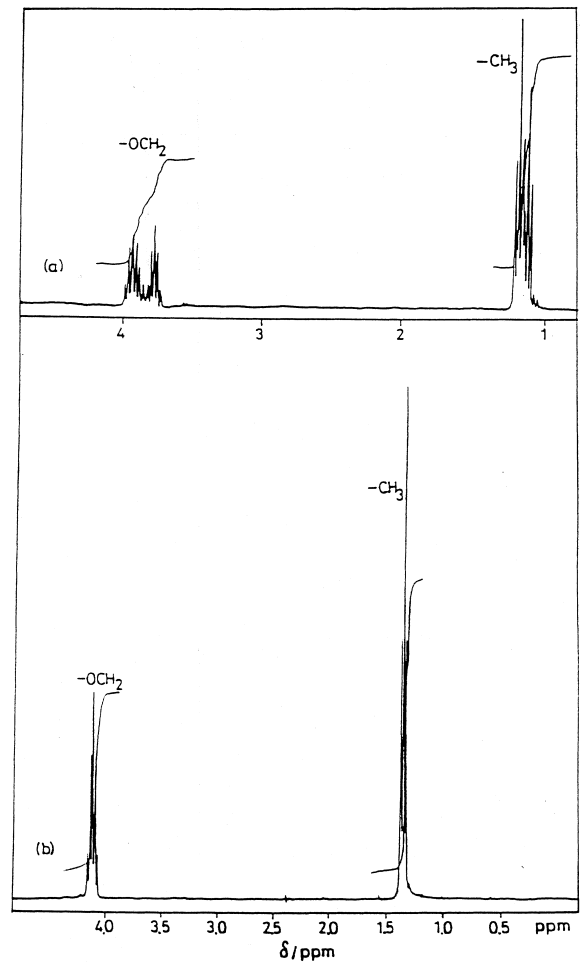

Fig. 6. ^{1}H NMR spectra of (a) NH_4L^2 in D_2O and (b) **1b** in $CDCl_3$.

singlet corresponding to $-OCH_3$ groups at 3.70 ppm and for the $R = C_2H_5$ complex one quartet at 4.18 and one triplet at 1.28 ppm due to $-OC_2H_5$ groups as internal symmetry makes all the ligands equivalent.

Although the decoupled ^{31}P NMR spectra of the ligands (NH_4L^{1-2}) in D_2O exhibit one signal as expected, the complexes in $CDCl_3$ solvent display two signals near 85 and 100 ppm having an intensity ratio of approximately 1:2 due to the presence of more than one type of phosphorus center in the solution state. This may provide support in favor of the presence of disulfide species along with the dimeric complex as proposed in Scheme 1.

In dichloromethane the violet colored complexes exhibit multiple transitions in the UV–Vis region. In the visible region the complexes display two moderately intense bands and the higher energy band is associated with a shoulder at a further higher energy part of the spectra (Table 4, Fig. 3). Since the ruthenium ion is in the +4 oxidation state in the complexes, the bands may therefore be assigned as ligand to metal charge-transfer transitions from sulfur to the metal ion [48–52]. The direct comparisons of the solid state reflectance spectra of **1** with the solution absorption spectra (Fig. 3, Tables 2 and 4) reveal that the bands have been reasonably blue shifted while moving from the solid to solution state.

Table 4
Electronic spectral [a] and electrochemical [b] data

Compound	λ (nm) (ε (M^{-1} cm^{-1}))	M^{IV}–M^{III} couple E^0_{298} (V) (ΔE_p (mV))	n [c]	M^{III}–M^{II} couple E^0_{298} (V) (ΔE_p (mV))
1a	510 (2231), 419 (1930), 277 (12748), 248 (21167)	1.01 (120)	1.93	−0.44(120)
1b	514 (2038), 422 (1680), 278 (11423), 246 (19455)	0.91 (122)	2.11	−0.49(100)
$\mathbf{1a}^{2-}$	613, 400, 266			
$\mathbf{1b}^{2-}$	600, 350, 243			

[a] In dichloromethane at 298 K.
[b] Conditions: solvent, dichloromethane; supporting electrolyte, NEt_4ClO_4; reference electrode, SCE; solute concentration, 10^{-3} M; working electrode, platinum. Cyclic voltammetric data: scan rate, 50 mV s^{-1}; $E^0_{298} = 0.5(E_{pc} + E_{pa})$ where E_{pc} and E_{pa} are the cathodic and anodic peak potentials respectively.
[c] $n = Q/Q'$ where Q' is the calculated Coulomb count for a two-electron transfer and Q that found after exhaustive electrolysis of $\sim 10^{-2}$ mol of solute.

The observed shift in band maxima on switching from solid to solution state supports the existence of different species in the solution state as shown in Scheme 1.

The strong bands in the UV region (Fig. 3) may be due to ligand centered transitions as the free ligands also exhibit a strong band in the same region (NH_4L^1, 236 nm and NH_4L^2, 237 nm in H_2O).

Electron-transfer properties of the complexes were studied in dichloromethane solvent by cyclic voltammetry using a platinum working electrode in the range ± 2.0 V versus a saturated calomel electrode (SCE) (tetraethyl ammonium perchlorate as electrolyte, 298 K). Representative voltammograms are shown in Fig. 7 and the reduction potentials are given in Table 4. The complexes display two reversible reductive couples and the separation between the two $E_{1/2}$ values is found to be ~ 1.4 V (Fig. 7, Table 4). The two-electron nature of the first couple (Fig. 7, couple I) is confirmed with the help of constant-potential coulometry (Table 4). The two-electron nature of the second couple (Fig. 7, couple II) at the negative side of SCE is determined by direct comparison of its differential pulse voltammogram peak height with that of the previous two-electron process (confirmed by coulometric experiment). The reduction potentials are observed to be lower for the complex having the ethoxy group (**1b**) as compared to the methoxy complex (**1a**).

The responses at positive and negative potentials are respectively assigned to ruthenium(IV)–ruthenium(III) and ruthenium(III)–ruthenium(II) couples as in Eqs. (2) and (3).

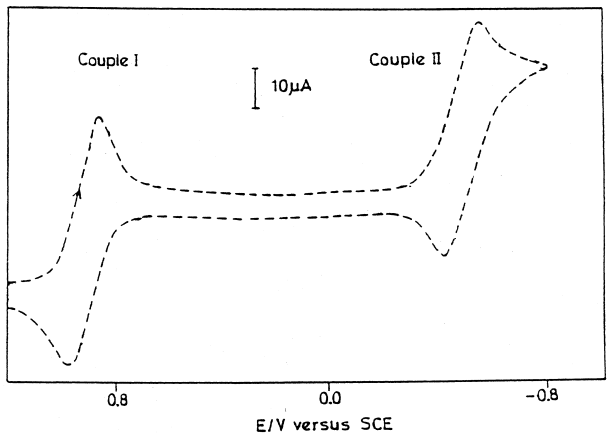

Fig. 7. Cyclic voltammograms of **1b** in dichloromethane at 298 K.

$$[\{(RO)_2PS_2\}_2Ru^{IV}(\mu\text{-}S)_2Ru^{IV}\{S_2P(OR)_2\}_2] + 2e^- \rightleftharpoons [\{(RO)_2PS_2\}_2Ru^{III}(\mu\text{-}S)_2Ru^{III}\{S_2P(OR)_2\}_2]^{2-} \quad (2)$$

$$[\{(RO)_2PS_2\}_2Ru^{III}(\mu\text{-}S)_2Ru^{III}\{S_2P(OR)_2\}_2]^{2-} + 2e^- \rightleftharpoons [\{(RO)_2PS_2\}_2Ru^{II}(\mu\text{-}S)_2Ru^{II}\{S_2P(OR)_2\}_2]^{4-} \quad (3)$$

It may be noted that the free ligands (NH_4L^{1-2}) do not show any redox activities within the specified potential range. Here the difference in potential between the two successive reduction processes is found to be ~ 1.4 V (Table 4) which is in good agreement with the earlier observed potential differences (1.3–1.4 V) between the two successive reduction processes $Ru^{IV/III}$–$Ru^{III/II}$ in other complexes [53–55].

Electrochemical reductions (constant-potential coulometry) of the complexes at 0.5 V versus SCE in dichloromethane solvent using a platinum gauze working electrode under a dinitrogen atmosphere result in a sharp color change from pink to greenish yellow. The observed Coulomb counts correspond to two-electron transfer (Table 4). The resulting reduced $[\{(RO)_2PS_2\}_2Ru^{III}(\mu\text{-}S)_2Ru^{III}\{S_2P(OR)_2\}_2]^{2-}$ species display voltammograms which are superposable on those of the corresponding starting complexes, which imply that the reductions here may be stereoretentive in nature [56]. When the same reduced solutions are reoxidized coulometrically at a potential 100 mV positive to the corresponding E_{pa} of the M^{III}/M^{IV} couple, the starting violet colored tetravalent complexes are formed quantitatively. The reduced species are not stable enough to be isolated in the solid state even at 273 K, however, we have managed to check the EPR spectra of the reduced complexes at 77 K and to record the qualitative electronic spectra. Since the reduced complexes are observed to be EPR silent even at 77 K, it may therefore be assumed that the two ruthenium(III) centers in the complexes are antiferromagnetically coupled [57]. In dichloromethane solvent, the complexes display two sulfur to metal charge transfer transitions in the visible region (Fig. 8, Table 4) and one ligand based transition in the UV region (Table 4).

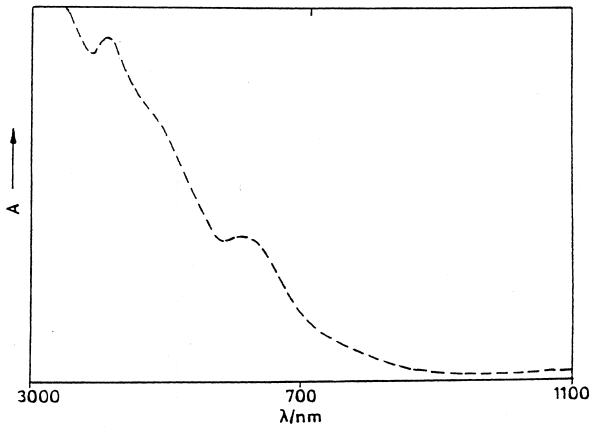

Fig. 8. Electronic spectrum of coulometrically reduced complex of $[\{(MeO)_2PS_2\}_2Ru^{III}(\mu\text{-}S)_2Ru^{III}\{S_2P(OMe)_2\}_2]^{2-}$ (**1a**$^{2-}$) in dichloromethane.

Coulometric reductions of the ruthenium complexes at -0.7 V versus SCE result in light blue colored reduced species. The resulting reduced complexes $[\{(RO)_2PS_2\}_2Ru^{II}(\mu\text{-}S)_2Ru^{II}\{S_2P(OR)_2\}_2]^{4-}$ are very unstable. On contact with a small amount of air, the complexes are oxidized immediately to the trivalent species, therefore no further study was made in this direction. The low $Ru^{III/II}$ potentials (~ -0.5 V) and the tetraanionic nature of the second reduced species might be responsible for their spontaneous aerial oxidation to the higher congeners.

The complexes can also be reduced chemically to the trivalent congeners by hydrazine hydrate. Although the greenish-yellow colored first step reduced species $[\{(RO)_2PS_2\}_2Ru^{III}(\mu\text{-}S)_2Ru^{III}\{S_2P(OR)_2\}_2]^{2-}$ are stable on the coulometric time scale and can even be generated by chemical means, all our attempts to isolate the first step reduced species in the pure solid state have failed. Further investigations are in progress in the direction of developing the first step reduced species, $[\{(RO)_2PS_2\}_2Ru^{III}(\mu\text{-}S)_2Ru^{III}\{S_2P(OR)_2\}_2]^{2-}$, particularly in the absence of any disulfide product in order to obtain direct evidence in favor of dimer formation.

4. Conclusions

We have observed that the reactions of dialkyldithiophosphate ligands with $RuCl_3\cdot 3H_2O$ result in paramagnetic tris ruthenium complexes $\{(RO)_2PS_2\}_3Ru^{III}$ (**1**) in the solid state, however, in solution the complexes exist predominantly in the dimeric form, $[\{(RO)_2PS_2\}_2Ru^{IV}(\mu\text{-}S)_2Ru^{IV}\{S_2P(RO)_2\}_2]$. The tetravalent dinuclear complexes are susceptible to facile stereoretentive electrochemical reductions to the corresponding trivalent and bivalent dinuclear congeners $[\{(RO)_2PS_2\}_2Ru^{III}(\mu\text{-}S)_2Ru^{III}\{S_2P(RO)_2\}_2]^{2-}$ and $[\{(RO)_2PS_2\}_2Ru^{II}(\mu\text{-}S)_2Ru^{II}\{S_2P(RO)_2\}_2]^{4-}$ respectively. The bivalent species are found to be unstable whereas the trivalent complexes are stable on the coulometric time scale but isolation in the pure solid state has not been successful.

Supplementary data

Supplementary data are available from the Cambridge Crystallography Data Centre, 12 Union Road, Cambridge CB2 1EZ, UK

Acknowledgements

Financial support received from the Department of Science and Technology, New Delhi, India, is gratefully acknowledged. The X-ray structural studies of **1a** and **1b** were carried out at the National Single Crystal Diffractometer Facilities, Indian Institute of Technology, Bombay and Department of Inorganic Chemistry, Indian Association for the Cultivation of Science, Calcutta, India respectively. Special acknowledgement is made to the Regional Sophisticated Instrumental Center, RSIC, Indian Institute of Technology, Bombay for providing NMR and EPR facilities.

References

[1] D.J. Duffy, L.H. Pignolet, Inorg. Chem. 13 (1974) 2045.
[2] K.W. Given, B.M. Mattson, L.H. Pignolet, Inorg. Chem. 15 (1976) 3152.
[3] B.M. Mattson, L.H. Pignolet, Inorg. Chem. 16 (1977) 488.
[4] L.H. Pignolet, D.J. Duffy, L. Que Jr., J. Am. Chem. Soc. 95 (1973) 289.
[5] L.J. Mathew, L.H. Pignolet, Inorg. Chem. 18 (1979) 3626.
[6] A.M. Bond, L. Martin, Coord. Chem. Rev. 54 (1984) 23.
[7] D. Coucouvanis, Prog. Inorg. Chem. 26 (1979) 301.
[8] K.W. Given, B.M. Mattson, G.L. Miessler, L.H. Pignolet, J. Inorg. Nucl. Chem. 39 (1977) 1309.
[9] C.L. Raston, A.W. White, J. Chem. Soc., Dalton Trans. (1975) 2418.
[10] J.V. Kingston, G. Wilkinson, J. Inorg. Nucl. Chem. 28 (1966) 2709.
[11] A.R. Hendrickson, J.M. Hope, R.L. Martin, J. Chem. Soc., Dalton Trans. (1976) 2032.
[12] C.L. Raston, A.W. White, J. Chem. Soc., Dalton Trans. (1975) 2405.
[13] C.L. Raston, A.W. White, J. Chem. Soc., Dalton Trans. (1975) 2422.
[14] A. Pramanik, N. Bag, G.K. Lahiri, A. Chakravorty, J. Chem. Soc., Dalton Trans. (1990) 3823.
[15] A. Pramanik, N. Bag, G.K. Lahiri, A. Chakravorty, Inorg. Chem. 30 (1991) 410.
[16] K.D. Keerthi, B.K. Santra, G.K. Lahiri, Polyhedron 17 (1998) 1387.
[17] G.A. Thakur, K. Narayanaswamy, G.K. Lahiri, Indian J. Chem. 35A (1996) 379.
[18] B.K. Santra, G.K. Lahiri, J. Chem. Soc., Dalton Trans. (1997) 129.
[19] A. Pramanik, N. Bag, G.K. Lahiri, A. Chakravorty, J. Chem. Soc., Dalton Trans. (1992) 101.
[20] N. Bag, G.K. Lahiri, A. Chakravorty, J. Chem. Soc., Dalton Trans. (1990) 1557.
[21] A. Pramanik, N. Bag, D. Ray, G.K. Lahiri, A. Chakravorty, J. Chem. Soc., Chem. Commun. (1991) 139.
[22] P.S. Rao, G.A. Thakur, G.K. Lahiri, Indian J. Chem. 35A (1996) 946.

[23] B.K. Santra, G.A. Thakur, P. Ghosh, A. Pramanik, G.K. Lahiri, Inorg. Chem. 35 (1996) 3050.
[24] B.K. Santra, P. Munshi, G. Das, P. Bharadwaj, G.K. Lahiri, Polyhedron 18 (1999) 617.
[25] S.S. Kulkarni, B.K. Santra, P. Munshi, G.K. Lahiri, Polyhedron 17 (1998) 4365.
[26] C.K. Jorgensen, Acta Chem. Scand. 16 (1962) 1048.
[27] M. Schroder, T.A. Stephenson, in: G. Wilkinson (Ed.), Comprehensive Coordination Chemistry, vol. 4, Pergamon, 1987, p. 430.
[28] W.P. Griffith, in: G. Wilkinson (Ed.), Comprehensive Coordination Chemistry, vol. 4, Pergamon, 1987, p. 603.
[29] M. Schroder, in: R.B. King (Ed.), Encyclopedia of Inorganic Chemistry, vol. 5, Wiley, New York, 1994, p. 2837.
[30] J.L. Lefferts, K.C. Mollouy, J.J. Zuckerman, I. Haituc, C. Guta, D. Ruse, Inorg. Chem. 19 (1980) 1662.
[31] D.T. Sawyer, A. Sobkowick, J.L. Roberts Jr., Electrochemistry for Chemists, Wiley, New York, 2nd edn., 1995.
[32] A.C.T. North, D.C. Phillips, F.S. Mathews, Acta Crystallogr., Sect. A 24 (1968) 351.
[33] G.M. Sheldrick, SHELXTL, Version 5.03, Siemens Analytical X-ray Instruments Inc., Madison, WI, 1994.
[34] C.K. Johnson, ORTEP, Report ORNL-5138, Oak Ridge National Laboratory, Oak Ridge, TN, 1976.
[35] N. Bag, G.K. Lahiri, S. Bhattacharya, L.R. Falvello, A. Chakravorty, Inorg. Chem. 27 (1988) 4396.
[36] B.K. Santra, M. Menon, C.K. Pal, G.K. Lahiri, J. Chem. Soc., Dalton Trans. (1997) 1387.
[37] S.L. Lawton, Inorg. Chem. 10 (1971) 328.
[38] D.F. Lewis, S.J. Lippard, J.A. Zubieta, Inorg. Chem. 11 (1972) 823.
[39] S.R. Fletcher, A.C. Skapski, J. Chem. Soc., Dalton Trans. (1972) 635.
[40] C.L. Raston, A.W. White, J. Chem. Soc., Dalton Trans. (1975) 2405.
[41] L.H. Pignolet, Inorg. Chem. 13 (1974) 2051.
[42] S.L. Lawton, G.T. Kakotailo, Inorg. Chem. 8 (1969) 2410.
[43] J.F. McConnell, V. Kastalsky, Acta Crystallogr. 22 (1967) 853.
[44] K. Kirschbaum, U. Bonnighausen, E. Gesing, K. Greiwe, U. Kuhlmann, H. Strasdeit, B. Krebs, G. Henkel, Z. Naturforsch., Teil B 45 (1990) 245.
[45] G.K. Lahiri, S. Bhattacharya, B.K. Ghosh, A. Chakravorty, Inorg. Chem. 26 (1987) 4324.
[46] R. Hariram, B.K. Santra, G.K. Lahiri, J. Organomet. Chem. 540 (1997) 155.
[47] L.L. Costanzo, I. Fragala, S. Giuffrida, G. Condorelli, Inorg. Chim. Acta 28 (1978) 19.
[48] N. Bag, A. Pramanik, G.K. Lahiri, A. Chakravorty, Inorg. Chem. 31 (1992) 40.
[49] M. Haga, E.S. Dodsworth, A.B.P. Lever, Inorg. Chem. 25 (1986) 447.
[50] A.B.P. Lever, P.R. Auburn, E.S. Dodsworth, M. Haga, W. Liu, M. Melnik, W.A. Nevin, J. Am. Chem. Soc. 110 (1988) 8076.
[51] B.K. Santra, G.K. Lahiri, J. Chem. Soc., Dalton Trans. (1997) 1883.
[52] A. Bharath, B.K. Santra, P. Munshi, G.K. Lahiri, J. Chem. Soc., Dalton Trans. (1998) 2643.
[53] B.M. Holligan, J.C. Jeffery, M.K. Norgett, E. Schatz, M.D. Ward, J. Chem. Soc., Dalton Trans. (1992) 3345.
[54] P. Ghosh, A. Pramanik, N. Bag, G.K. Lahiri, A. Chakravorty, J. Organomet. Chem. 454 (1993) 273.
[55] D.A. Bradwell, J.C. Jeffery, E. Schatz, E.E.M. Tilley, M.D. Ward, J. Chem. Soc., Dalton Trans. (1995) 825.
[56] R. Samanta, P. Munshi, B.K. Santra, N.A. Lokanath, M.A. Sridhar, J.S. Prasad, G.K. Lahiri, J. Organomet. Chem. 581 (1999) 311.
[57] B.K. Santra, G.K. Lahiri, J. Chem. Soc., Dalton Trans. (1998) 139.